



# Search for large extra spatial dimensions in Jets + Missing $E_T$ topologies

The DØ Collaboration  
URL: <http://www-d0.fnal.gov>  
(Dated: March 19, 2004)

A search for signals of extra spatial dimensions is performed using  $85 \text{ pb}^{-1}$  of data from  $p\bar{p}$  collisions at a center-of-mass energy of 1.96 TeV, collected by the DØ detector at the Fermilab Tevatron. The topologies analyzed consist of single jets and acoplanar jets with missing  $E_T$ . The data show good agreement with the standard model expectations; in absence of evidence for a signal from large extra dimensions, new limits on the fundamental Planck scale have been derived.

*Preliminary Results for Winter 2004 Conferences*

## I. INTRODUCTION

Topologies involving jets and missing transverse energy have been widely investigated in the past to search for signals of new phenomena in  $p\bar{p}$  collisions. In this note, searches for anomalies in the monojet and acoplanar jet topologies are reported, using  $85\text{ pb}^{-1}$  of data collected at a center-of-mass energy of 1.96 TeV by the upgraded DØ detector during Run II of the Fermilab Tevatron.

Theories of large extra dimensions (LED) have been proposed as a possible solution of the hierarchy problem. In a large class of models [1], the effect of the extra spatial dimensions is visible in our 4D world as the presence of a series of graviton (G) states (“Kaluza Klein tower”). At the Tevatron, gravitons can be produced recoiling against a quark or gluon jet [2]. The large number of kinematically accessible states compensating for the small gravitational coupling to give sizable cross sections. The resulting topology is monojet-like. Previous studies at Run I allowed limits to be set on the fundamental Planck scale  $M_D$ , as a function of the number  $n_D$  of extra dimensions: for  $n_D = 7$ , the limit is 0.6 TeV [3]. (Here and in the following, all limits are quoted at the 95% confidence level.)

## II. DATA SAMPLE AND PRESELECTION

This analysis is based on  $85\text{ pb}^{-1}$  of data collected between April and September 2003, where all major subdetectors are required to be fully functional. The trigger was specifically designed for the Jets + Missing  $E_T$  topologies. At the first level of trigger, there should be at least three trigger towers with  $E_T$  in excess of 5 GeV. At the second and third trigger levels, requirements are placed on  $\cancel{E}_T$ , the transverse energy missing from the reconstructed jets ( $\cancel{E}_T = |\sum_{jets} \vec{p}_T|$ ). The  $\cancel{E}_T$  thresholds are 20 and 30 GeV at Levels 2 and 3, respectively.

Electrons and jets are corrected for their respective energy scale; standard quality criteria are used to identify good electrons, muons and jets. Additional event quality criteria are applied. First, events with identified noise or malfunction in the calorimeter are rejected. Second, it is required that no jet failing quality cuts be reconstructed with  $p_T > 15\text{ GeV}/c$ . The inefficiencies introduced by these clean-up cuts were measured on independent samples of random beam crossing events and events from jet triggers. The total inefficiency introduced by these cuts is 3.4%.

To select a loose sample of signal-like events,  $\cancel{E}_T$  is required to be in excess of 40 GeV for the trigger efficiency to be high. Furthermore, the leading jet  $p_T$  is required to be larger than 80 GeV/ $c$ .

So far the sample is still dominated by QCD events with mismeasured jet transverse energy. Such mismeasurements can in particular be due to a wrong vertex choice. Fake monojet or even dijet events can also be caused by cosmic rays showering in the calorimeter. The improved tracking capabilities of the upgraded DØ detector can be used to largely reduce these backgrounds.

First the longitudinal position  $z$  of the vertex is restricted to ensure an efficient primary vertex reconstruction:  $|z| < 60\text{ cm}$ . This requirement introduced a 3.9% inefficiency as measured on a QCD sample. Next a comparison of the jet energy with its counterpart carried by charged particles is performed. The jet charged particle energy fraction CPF is calculated from tracks that are associated to the jet and that are compatible with originating from the primary vertex. It is defined as being the ratio of the sum of pT of those tracks to the jet ET. CPF is expected to be close to zero either if a wrong primary vertex was selected or if the jet is a fake one, in which case there should be no real charged tracks associated to it. The CPF distribution is shown in Fig. 1, for jets belonging to a QCD sample. In the following, a jet will be considered confirmed if its CPF is larger than 0.05.

The inefficiency of this jet confirmation procedure is determined using back-to-back dijet events from the QCD sample, with both jets required to be central ( $|\eta_{det}| < 1$ ) [6]. From the fractions of events with 0, 1 or 2 jets confirmed, it is deduced that the chosen vertex is the correct one in 99% of the cases, and that track confirmation of a jet then occurs at a rate of 98% within  $|\eta_{det}| < 1$ . It has been checked that this efficiency does not depend on the jet  $p_T$  within the range of interest.

Signal efficiencies and non-QCD standard model backgrounds have been evaluated using fully simulated and reconstructed Monte Carlo events. The jet energies received an additional smearing to take into account the different resolutions in data and Monte Carlo.

## III. STANDARD MODEL BACKGROUND SAMPLES

The main physics background arise from the production of a W or Z boson in association with jets when the boson decay leptonically. That includes in particular the irreducible background from Z boson plus jets production with the Z boson decaying to neutrinos, leading to the same monojet or acoplanar jet topology as that of the signal. Large samples of fully simulated events have been produced with ALPGEN interfaced with PYTHIA for the simulation of initial

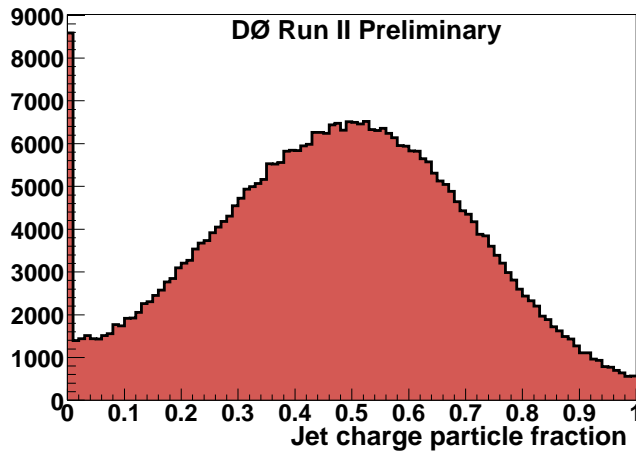


FIG. 1: Distribution of the charged particle fraction CPF for central jets.

and final state radiation, and of jet hadronization, with an average of 0.8 minimum bias events superimposed to simulate the typical instantaneous luminosity at which the data have been taken.

#### IV. SEARCH FOR SIGNAL OF EXTRA DIMENSIONS

##### A. Signal simulation

The event generator is based on code from J. Lykken and K. Matchev that implements the calculation of Ref. [2], and was adapted from the one used in Ref. [3]. The matrix elements of the following processes are calculated

$$q\bar{q} \rightarrow Gg,$$

$$qg \rightarrow Gq,$$

$$gg \rightarrow Gg,$$

and interfaced with PYTHIA 6.202, using the CTEQ5L PDF's. Samples of 10 000 signal events were fully simulated for  $n_D = 4, 5, 6$  and  $7$ , and for  $M_D = 0.6, 0.7$  and  $0.8$  TeV, with an average of 0.8 minimum bias events superimposed.

##### B. Trigger simulation

The analysis, as described in the next sections, requires a high  $p_T$  jet and large  $p_T$  imbalance. For such events, the main trigger inefficiency comes from the condition at the first level of trigger, especially for pure monojet events. This level 1 trigger efficiency was measured on a sample of real data events triggered by a muon in order to be unbiased with respect to calorimetric trigger conditions. Back-to-back dijet events from this sample have been used in the following way: for each jet, the number of trigger towers with transverse energy larger than 5 GeV and within  $\Delta R < 0.5$  of the jet axis is determined. The jet is considered having triggered the Level 1 condition if this number is equal to three or larger. Jets close to the triggering muon are excluded from this procedure.

##### C. Event selection

The selection cuts listed in Table I were applied to the events after the preselection described above. The kinematic cuts **C1**, **C2**, **C7**, **C8** and **C9** were directly taken from Ref. [3]. (For **C9**, the test in Ref. [3] was only applied to the second leading jet.)

The distributions of the variables used for the last three cuts are shown in figures 2, 3 and 4 before the corresponding cut has been applied. As expected, before  $\cancel{E}_T$  cut the background is dominated by QCD events while is it dominated by physics events at the end of the analysis.

TABLE I: Cuts applied in the monojet analysis, events remaining at each step, signal efficiency in percent for  $n_D = 6$  and  $M_D = 700$  GeV, and supporting figure.

cut applied	events left	efficiency (%)	Figure
preselection	358 120		
<b>C1:</b> leading jet $p_T > 150$ GeV/ $c$	38 556	8.3	
<b>C2:</b> leading jet $ \eta_{\text{det}}  < 1$ .	28 252	7.2	
<b>C3:</b> leading jet EMF $< 0.95$	28 014	7.2	
<b>C4:</b> leading jet CPF $> 0.05$	23 473	7.2	
<b>C5:</b> no electromagnetic object with $p_T > 10$ GeV/ $c$	22 963	7.1	
<b>C6:</b> no isolated muon with $p_T > 10$ GeV/ $c$	22 864	7.1	
<b>C7:</b> $\cancel{E}_T > 150$ GeV	150	6.5	Fig. 2
<b>C8:</b> second leading jet $p_{T2} < 50$ GeV/ $c$	91	5.6	Fig. 3
<b>C9:</b> minimum $\Delta\Phi_{(E_T, \text{jet})} > 30^\circ$	63	5.2	Fig. 4

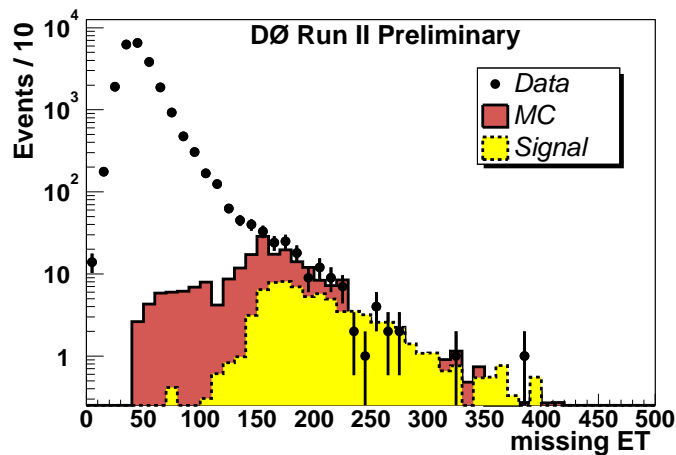


FIG. 2: Distribution of  $\cancel{E}_T$  after cuts **C1** to **C6** for data (points with error bars), for non-QCD standard model background (full histogram), and for signal Monte Carlo ( $n_D = 6$ ,  $M_D = 0.7$  TeV; dashed histogram).

## D. Backgrounds

### 1. Standard model backgrounds

The standard model background contributions to the selected monojet sample are listed in Table II. The main contributors are, as expected,  $Z \rightarrow \nu\bar{\nu} + \text{jet}(s)$ .

There is a deficit of almost  $3\sigma$  in the number of events observed compared to the SM background expectation. This analysis is however very sensitive to the jet energy scale. To investigate the effect of the associated uncertainties, it was repeated after applying to the simulation a JES modified by  $\pm$  one standard deviation of an error calculated as the quadratic sum of the data and Monte Carlo uncertainties. In terms of numbers of events, the discrepancy between data and SM background expectation is reduced to about  $1\sigma$ . The impact of the JES uncertainties on the  $\cancel{E}_T$  and  $p_{T1}$  distributions can be appreciated in Fig. 5.

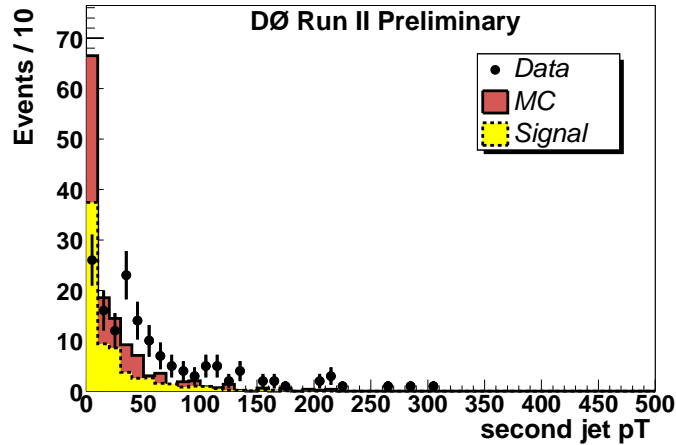


FIG. 3: Distribution of the second leading jet  $p_T$  after cuts **C1** to **C7** for data (points with error bars), for non-QCD standard model background (full histogram), and for signal Monte Carlo ( $n_D = 6$ ,  $M_D = 0.7$  TeV; dashed histogram).

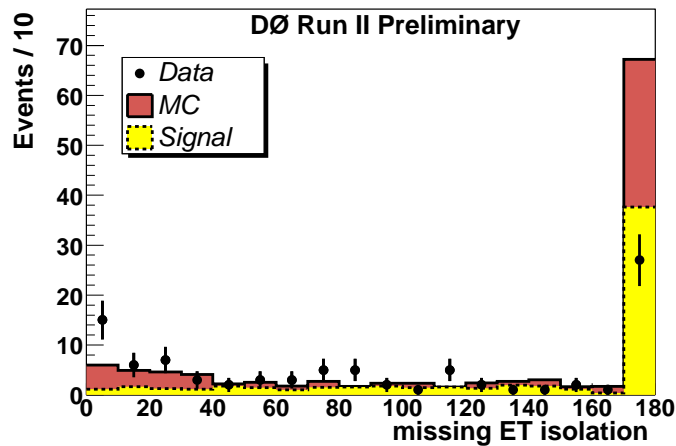


FIG. 4: Distribution of the minimum  $\Delta\Phi_{(E_T, \text{jet})}$  after cuts **C1** to **C8** for data (points with error bars), for non-QCD standard model background (full histogram), and for signal Monte Carlo ( $n_D = 6$ ,  $M_D = 0.7$  TeV; dashed histogram).

TABLE II: Standard model processes and numbers of events expected in the monojet analysis. The errors on the numbers of events expected in the individual channels are statistical only. For the total background, the first error is statistical, and the second accounts for the cross section uncertainties.

SM process	cross-section (pb)	events expected
$Z \rightarrow \nu\bar{\nu} + \text{jet}$	422	$32.1 \pm 3.4$
$Z \rightarrow \nu\bar{\nu} + \text{jet jet}$	144	$28.4 \pm 2.8$
$W \rightarrow \tau\nu + \text{jet}$	732	$13.3 \pm 2.6$
$W \rightarrow \tau\nu + \text{jet jet}$	255	$8.9 \pm 2.4$
$W \rightarrow \mu\nu + \text{jet}$	732	$5.8 \pm 1.7$
$W \rightarrow \mu\nu + \text{jet jet}$	255	$6.2 \pm 0.8$
$W \rightarrow e\nu + \text{jet}$	732	$4.1 \pm 1.6$
$W \rightarrow e\nu + \text{jet jet}$	255	$1.2 \pm 0.4$
$Z \rightarrow \tau\tau + \text{jet}$	72	0
$Z \rightarrow \mu\mu + \text{jet}$	72	$0.07 \pm 0.05$
$Z \rightarrow \mu\mu + \text{jet jet}$	26	$0.2 \pm 0.05$
total		$100.2 \pm 6.2 \pm 7.5$

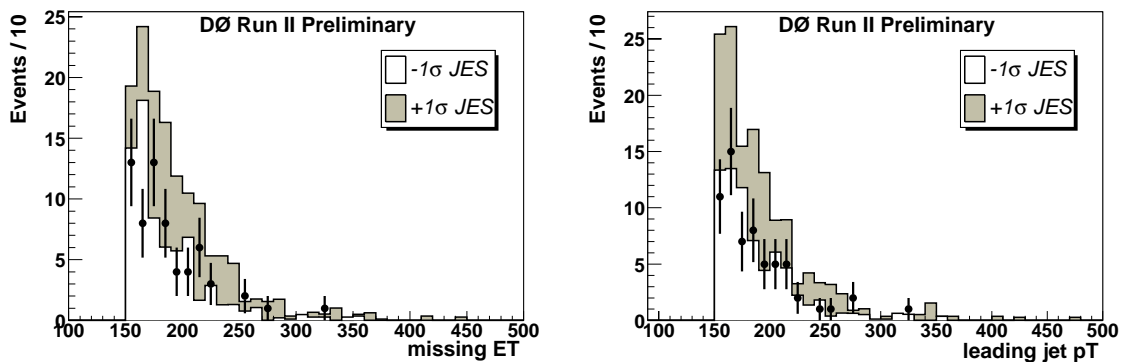


FIG. 5: In the monojet analysis, distributions of the missing  $E_T$  (left) and of the leading jet  $p_T$  (right) after all cuts for data (points with error bars) and for non-QCD standard model background (histogram). The shaded band in the latter indicates the effect of the jet energy scale uncertainties.

## 2. QCD background

Altogether, the standard model processes leave only little room (if any at all) for the QCD background. Several tests have been performed to estimate the probability for jets in high  $p_T$  QCD events to fluctuate such that the events would pass the selection criteria detailed above. It is estimated that the QCD background is small and it will be conservatively neglected in the derivation of limits.

## E. Results

### 1. Signal efficiency

The signal efficiency was evaluated using simulated events, taking into account the trigger efficiency and the known small differences between data and simulation. The results are displayed in Table III for various choices of model parameters, and in Table I at each step of the analysis for  $n_D = 6$  and  $M_D = 700$  GeV.

TABLE III: Signal efficiency and number of signal events expected for various choices of model parameters. The errors are statistical only.

$n_D$	$M_D$ (TeV)	efficiency (%)	events expected
4	0.6	$5.2 \pm 0.2$	$170 \pm 8$
4	0.7	$5.4 \pm 0.2$	$70.1 \pm 3.1$
4	0.8	$5.2 \pm 0.2$	$30.3 \pm 1.3$
5	0.6	$5.4 \pm 0.2$	$183 \pm 7$
5	0.7	$5.4 \pm 0.2$	$62.1 \pm 2.3$
5	0.8	$5.5 \pm 0.2$	$24.9 \pm 0.9$
6	0.6	$5.4 \pm 0.2$	$205 \pm 8$
6	0.7	$5.2 \pm 0.2$	$57.3 \pm 2.2$
6	0.8	$5.4 \pm 0.2$	$20.4 \pm 0.8$
7	0.6	$4.8 \pm 0.2$	$215 \pm 10$
7	0.7	$4.8 \pm 0.2$	$53.7 \pm 2.4$
7	0.8	$4.7 \pm 0.2$	$15.8 \pm 0.7$

### 2. Systematic errors

The main experimental systematic errors are fully correlated between signal and SM backgrounds:

- a 6.5% uncertainty on the integrated luminosity;
- the uncertainties in the data and Monte Carlo jet energy scales. These are added in quadrature and yield a 20% relative uncertainty on the signal efficiency, and a  $^{+50}_{-30}\%$  uncertainty on the SM background prediction.

The signal cross sections were evaluated using the CTEQ5L PDF's. To estimate the uncertainty related to the PDF choice, these cross sections have been recalculated with GRV98L0 and MRSTc-g98. The result is an increase by 8% and 11%, respectively, with respect to the default choice. Conservatively, no systematic error associated to the PDF choice was assigned to derive the final results.

### 3. Limits on model parameters

From the absence of excess in the data with respect to the expectation from SM backgrounds, lower limits on  $M_D$  are obtained as a function of  $n_D$ , using the LEP  $CL_s$  approach. The results, given in Table IV, improve on those obtained with Run I data [3]. The limit is illustrated in Fig.6 together with the limits from CDF Run I with no K-factor [4] and the most stringent limits from LEP [5].

Since the number of observed events is less than the number of expected events, although well within the systematics uncertainties, it is important to compare the actual limits to expectations. Expressed in terms of number of signal events, the limit is 84 events. From ensemble tests, taking into account the expected number of events and the uncertainties, the median limit is 111.4 events, the average 123.8 events and the RMS 28.1 events.

TABLE IV: Lower limits on  $M_D$ , for various choices of  $n_D$ , with the limits from CDF with no K-factor [4] and the most stringent limits from LEP [5]

$n_D$	$M_D$ lower limit (TeV)	CDF limit (TeV)	LEP limit (TeV)
4	0.68	0.77	0.91
5	0.67		0.76
6	0.66	0.73	0.65
7	0.68		0.51

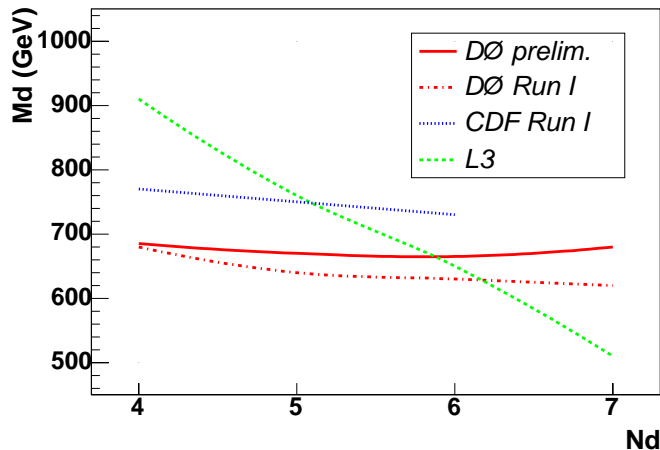


FIG. 6: The limit on the fundamental Planck scale  $M_D$  for various number of extra dimensions  $N_D$  (full line), together with the CDF (dotted line) and DØ (dashed-dotted line) Run I limits and the most stringent LEP limit (dashed line).

### Acknowledgments

We thank the staffs at Fermilab and collaborating institutions, and acknowledge support from the Department of Energy and National Science Foundation (USA), Commissariat à L'Énergie Atomique and CNRS/Institut National

de Physique Nucléaire et de Physique des Particules (France), Ministry for Science and Technology and Ministry for Atomic Energy (Russia), CAPES, CNPq and FAPERJ (Brazil), Departments of Atomic Energy and Science and Education (India), Colciencias (Colombia), CONACyT (Mexico), Ministry of Education and KOSEF (Korea), CONICET and UBACyT (Argentina), The Foundation for Fundamental Research on Matter (The Netherlands), PPARC (United Kingdom), Ministry of Education (Czech Republic), Natural Sciences and Engineering Research Council and West-Grid Project (Canada), BMBF (Germany), A.P. Sloan Foundation, Civilian Research and Development Foundation, Research Corporation, Texas Advanced Research Program, and the Alexander von Humboldt Foundation.

- 
- [1] N. Arkani-Hamed, S. Dimopoulos and G. Dvali, Phys. Lett. **B 429** (1998) 263.  
 [2] G. Giudice, R. Rattazzi and J.D. Wells, Nucl. Phys. **B 544** (1999) 3.  
 [3] DØ Collaboration, V.M. Abazov *et al.*,  
 “Search for Large Extra Dimensions in the Monojet + Missing  $E_T$  Channel with the DØ Detector”,  
 Phys. Rev. Lett. **90** (2003) 251802.  
 [4] CDF Collaboration, D. Acosta *et al.*, “Search for Kaluza-Klein Graviton Emission in  $p$  anti- $p$  Collisions at  $\sqrt{s} = 1.8$  TeV using the Missing Energy Signature”, FERMILAB-PUB-03/285-E  
 [5] L3 Collaboration, P. Achard *et al.*, *Single- and Multi-Photon Events with Missing Energy in the  $e^+e^-$  Collisions at LEP*, CERN-EP/2003-068, accepted by Phys. Lett. B.  
 [6]  $|\eta_{\text{det}}|$  is the pseudo-rapidity as measured from the detector centre, a jet with  $|\eta_{\text{det}}| < 1$  is mostly contained in the central calorimeter.